

## Robust Self-cleaning Surfaces that Function when Exposed to either Air or Oil

**Authors:** Yao Lu<sup>1</sup>, Sanjayan Sathasivam<sup>1</sup>, Jinlong Song<sup>2</sup>, Colin R. Crick<sup>3</sup>, Claire J. Carmalt<sup>1</sup> and Ivan P. Parkin<sup>1\*</sup>

### Affiliations:

<sup>1</sup> Department of Chemistry, University College London, 20 Gordon Street, London, WC1H 0AJ, UK.

<sup>2</sup> Key Laboratory for Precision and Non-traditional Machining Technology of Ministry of Education, Dalian University of Technology, Dalian, 116024, People's Republic of China.

<sup>3</sup> Department of Chemistry, Imperial College London, South Kensington Campus, London, SW7 2AZ, UK.

\*Correspondence to: [i.p.parkin@ucl.ac.uk](mailto:i.p.parkin@ucl.ac.uk) (I. P. Parkin).

**Abstract:** Superhydrophobic self-cleaning surfaces are based on the surface-micro/nano-morphologies, however, such surfaces are mechanically weak and stop functioning when exposed to oil. We have created an ethanolic suspension of perfluorosilane coated titanium dioxide nanoparticles which forms a paint that can be sprayed, dipped or extruded onto both hard and soft materials, to create a self-cleaning surface that functions even on emersion in oil. Commercial adhesives were used to bond the paint to various substrates and promote robustness. These surfaces maintained their water repellency after finger-wipe, knife-scratch and even 40 abrasion cycles with sandpaper. The formulations developed can be used on clothes, paper, glass and steel for a myriad of self-cleaning applications.

**One Sentence Summary:** Robust self-cleaning surfaces were formed using a nanoscale paint on a flexible substrate that function even after either mechanical damage or oil contamination.

**Main Text:** Artificial self-cleaning surfaces work through extreme water repellence (superhydrophobicity), such that water forms near spherical shapes that roll on the surface; the rolling motion picks up and removes dirt, viruses and bacteria (1-3). To achieve near spherical water droplets the surfaces must be highly textured (rough) combined with extremely low water affinity (waxy) (4, 5). The big drawback of these artificial surfaces is that they are readily abraded (6-8), sometimes with little more than brushing with a tissue, and readily contaminated by oil (9-11). We report here a facile method for making superhydrophobic surfaces from both soft (cotton, paper) and hard (metal, glass) materials. The process uses dual scale nanoparticles of titanium dioxide (TiO<sub>2</sub>) that are coated with perfluorooctyltriethoxysilane. We created an ethanol-based suspension that can be sprayed, dipped or painted onto surfaces to create a resilient water repellent surface. By combining the paint and adhesives, we created a superhydrophobic surface that showed resilience and maintained its performance after various types of damage, including finger-wipe, knife-scratch and multiple abrasion cycles with sandpaper. This method can also be used for components that require self-cleaning and lubricating such as bearings and gears, to which, superamphiphobic (repels oil and water) surfaces (9-11) are not applicable.

A paint was created by mixing two different size ranges of TiO<sub>2</sub> nanoparticles (*ca* 60-200 nm and *ca* 21 nm) in an ethanol solution containing perfluorooctyltriethoxysilane (12). Scanning electron microscopy (SEM) and transmission electron microscopy (TEM) of the constituent

particles of the paint (Fig. 1A) show the dual scale nature of the TiO<sub>2</sub> nanoparticles. X-ray photoelectron spectroscopy (XPS) (Fig. 1B) showed that the titanium dioxide particles were coated with perfluorooctyltriethoxysilane.

Many different coating methods were used to create the water repellent surfaces, including an artist's spray-gun to coat hard substrates such as glass and steel, dip-coating for cotton wool and a syringe (Movie S1) to extrude the paint onto filter paper. After allowing the ethanol to evaporate for *ca* 180 s at room temperature, the treated areas of the substrates supported water as near spherical droplets while the untreated parts were readily wetted (it required *ca* 30 minutes for the ethanol to fully evaporate from cotton wool and filter paper at room temperature) (Fig. S1). X-ray diffraction (XRD) (Fig. 1C) was used to analyse the coatings on hard and soft substrates. The diffraction peaks show the expected patterns for nanoscaled TiO<sub>2</sub>.

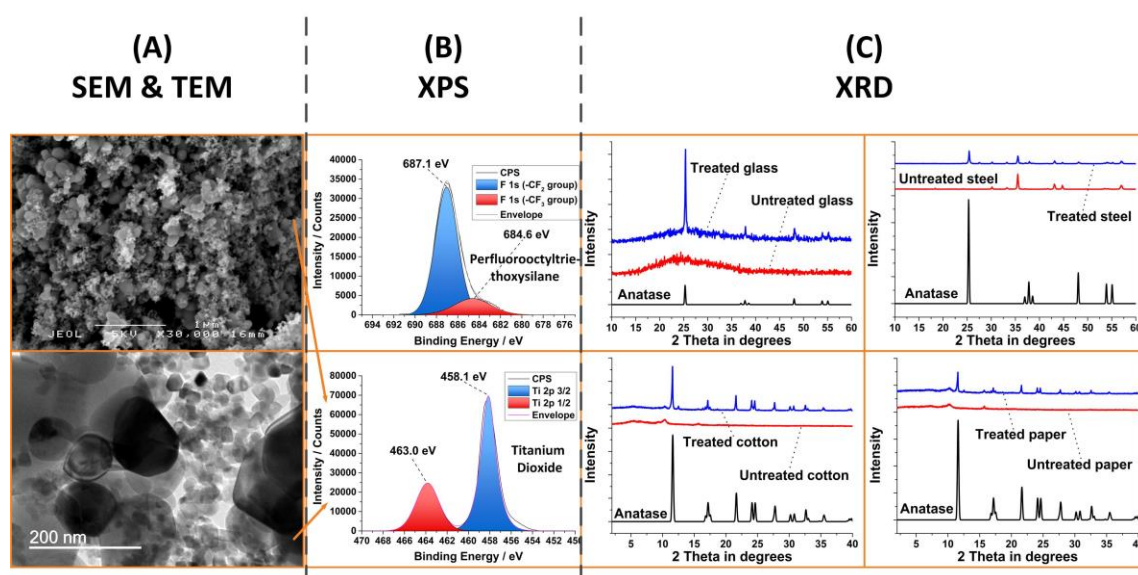


**Fig. 1 Paint characterizations.** (A) SEM (top) and TEM (bottom) of the constituent nanoparticles in the paint, sizes varied from *ca* 60 nm to 200 nm for the TiO<sub>2</sub> nanoparticles (Aldrich), while *ca* 21 nm in size refers to P25. (B) XPS of the paint, where F refers to perfluorooctyltriethoxysilane and Ti refers to TiO<sub>2</sub>. (C) XRD patterns of treated and untreated substrates compared with the respective standard patterns for TiO<sub>2</sub> anatase (note the P25 particles had as expected a small rutile component).

On a surface that shows water repellence, water droplets tend to bounce instead of wetting the surface (13, 14). However, for soft substrates, extreme superhydrophobicity is required to achieve the bouncing phenomenon as the water droplets tend to be trapped onto the threads of the substrates (i.e. cotton wool) (15). Fig. S2 shows the water dropping tests on untreated glass, steel, cotton wool and filter paper, which were readily wetted (the contact moment of the water droplets and the solid surfaces is defined as 0). Fig. 2 shows the water bouncing process on dip-coated glass, steel, cotton wool and filter paper surfaces. Water droplets completely leave the surface without wetting or even contaminating the surfaces (the water was dyed blue to aid visualisation), indicating that the surfaces were superhydrophobic. Movie S2 compares the water impacting behaviour between untreated and treated glass, steel, cotton wool and filter paper, respectively. Movie S3 shows the effect of artificial rain on the treated surfaces,

the drop sizes varied with random impacting velocities, and all of the droplets could not wet the treated surfaces.

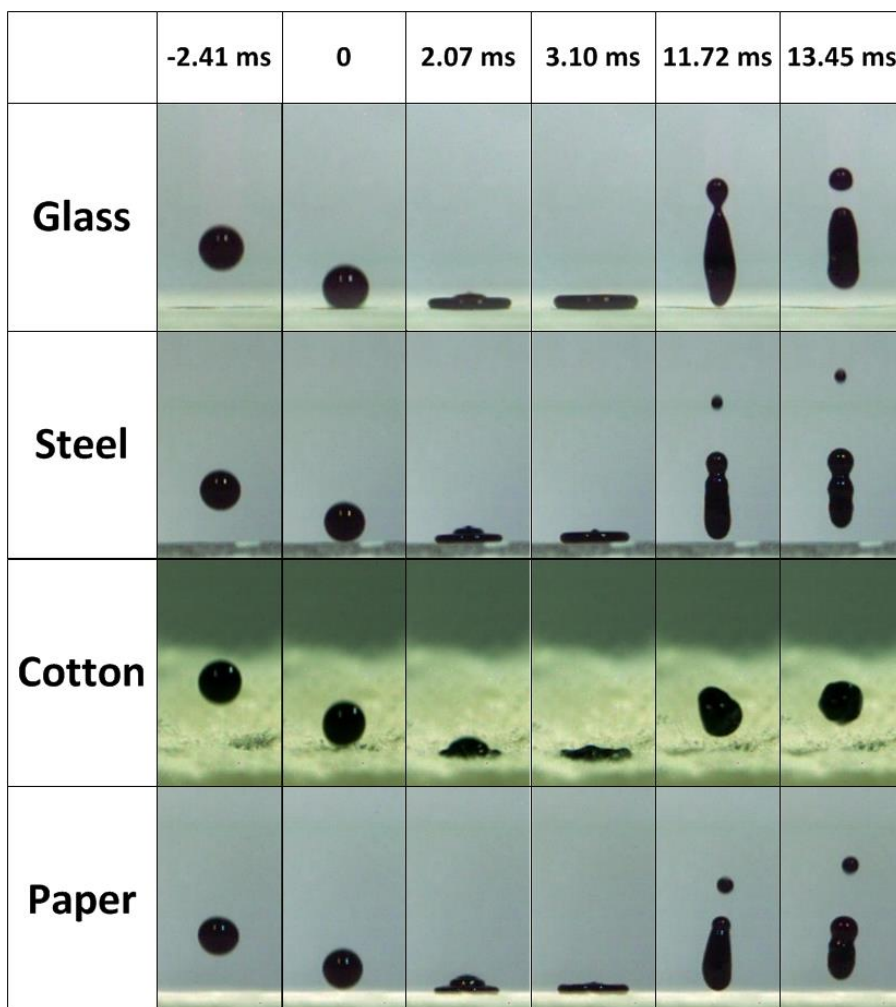


**Fig. 2 Time-lapse photographs of water droplets bouncing on the treated glass, steel, cotton wool and filter paper surfaces (droplet size:  $ca\ 6.3 \pm 0.2\ \mu\text{L}$ ).**

The paint had good self-cleaning properties when applied on various substrates, especially for soft porous materials, such as those used in making clothes and paper. The coated surfaces show water-proofing properties from the water bouncing and artificial rain tests. Further tests on cotton wool and filter paper are shown in Fig. S3 (the experimental scheme) and Fig. S4 (the experimental results). Fig. S4 A and B shows that the dip-coated cotton wool inserted into the methylene blue dyed water formed a negative meniscus on the solid-liquid-vapour interfaces due to hydrophobicity (16). The cotton wool was removed from the water, and it remained fully white with no trace of contamination by the dyed water (Fig. S3). Fig. S4 C and D shows a dirt removal test when an artificial dust (MnO powder) was put on the spray-coated filter paper, which was then cleaned by pouring water. The untreated piece of filter paper (placed below) was wet and polluted by the dirt while the treated piece stayed dry and clean (Fig. S3). Movie S4 shows the self-cleaning tests on the dip-coated cotton wool and spray-coated filter paper; Movie S5 shows a time-lapsed video clip of water droplets (dyed blue) staying on the dip-coated cotton

wool and syringe-coated filter paper for 10 min, and neither the cotton wool nor the filter paper had blue left after the droplets were removed. These tests indicate that the soft substrates (cotton and paper) gained the non-wetting and self-cleaning properties after treating with the paint. Dirt removal tests were also carried out on dip-coated glass and steel surfaces, as shown in Fig. S4 E and F, the droplet took the dirt (MnO powder) away and the surfaces were cleaned along the path of the water droplet movement. Movie S6 shows the self-cleaning property of dip-coated glass and steel surfaces in a high-speed motion capture.

Very few reports have shown any self-cleaning tests in oil as superhydrophobic surfaces normally lose their water repellency when even partially contaminated by oil. This is because the surface tension of the oil is lower than that of water, resulting in the oil penetrating through the surfaces. Making superamphiphobic surfaces (that repel both water and oils) is an effective way to solve this problem (9, 10, 17). However, there are many instances that require both self-cleaning from water repellency and a smooth coating of oil, such as lubricating bearings and gears, under these conditions, superamphiphobic surfaces cannot be used as they will also repel lubricating oils. Fig. S5 graphically presents the self-cleaning tests of the painted surfaces after oil (hexadecane) contamination and immersion. Fig. S6 shows that water droplets still formed “marbles” on the dip-coated surface when immersed in oil, rather than forming a two layer system (Fig. S5A), thus indicating that the surfaces will retain their self-cleaning properties after being immersed in oil. For example on the untreated areas of a glass slide, water droplets spread and wet the surfaces. Movie S7 shows water dropped on the dip-coated and untreated surfaces immersed in oil. Fig. 3A shows the side view of a water droplet that formed a sphere at the oil-solid interface without wetting a spray-coated surface, the droplet then rolled off from the surface. Fig. 3, B and C, shows that the water droplets slipped off from the spray-coated surface that was contaminated by oil (hexadecane), indicating self-cleaning was retained even after oil-contamination (Fig. S5B, Movie S8). Fig. 3, D to F, shows a dirt removal test on the spray-coated surfaces both in oil and in air. The treated surface was fully contaminated by oil, and then partly inserted into oil; dirt (MnO powder) was also put partly in oil and air onto the surface. Water was dropped to remove the dirt both in air and oil (Fig. S5C, Movie S9). This was to test the dirt-removal properties of the oil-contaminated painted surface both in air and under oil. For further dirt-removal tests on oil-contaminated painted surfaces, we used soil, household dust and cooking oil from actual conditions and repeated the experiments shown in Fig. S5C. Fig. S7 shows that soil and dust were removed by water from the dip-coated surfaces immersed either in hexadecane or cooking oil.

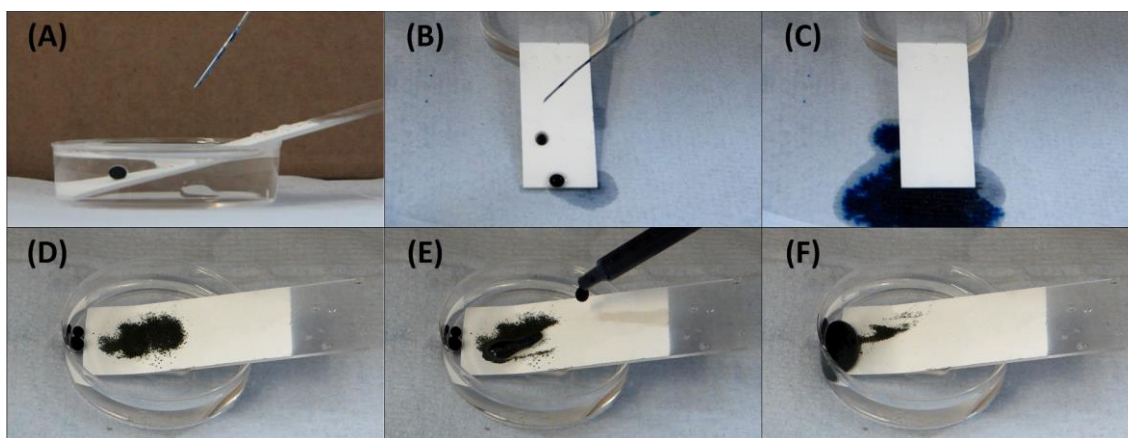


**Fig. 3 Self-cleaning tests after oil-contaminations.** (A) Water droplet was repelled by the treated surface when immersed in oil (hexadecane); (B) and (C) show the treated surface retained its water repellent property even after being contaminated by oil; (D) to (F) shows the dirt removal test in oil-solid-vapour interfaces, dirt was put partly in oil and air, the surface was contaminated by oil, water was dropped onto the surface and this removed the dirt both in air and oil.

When the treated surfaces were immersed in oil, the oil gradually penetrated into the surface, so the water droplets were supported by both oil and the surface structures and were still marble-shaped (Fig. S6). In this condition, the self-cleaning behaviour in oil is similar to that in air (18-20), thus the treated surfaces retained the water repellent and dirt removal properties when immersed in oil (Fig. 3, D to F). In air, when the treated surfaces were contaminated by oil, the surface structures locked the oil as a lubricating fluid and a slippery state was then achieved (21-24). Dirt was removed from the treated surfaces by simply passing water over the surface. For these reasons, the treated surfaces retained its self-cleaning properties when being contaminated by oil.

Low surface robustness is the main issue limiting the widespread application of superhydrophobic coatings as the surface roughness is usually at the micro or nano-scale and is mechanically weak and readily abraded (25). This surface roughness is partially protected by soft substrates, such as cotton wool and filter paper, due to their inherent flexibility (6, 26) and ability to reduce direct friction between the coating and the surface. However, on hard substrates like glass, nano structures are easily destroyed or removed. We developed a method to bond the self-cleaning coatings to the substrates using adhesives, and the idea was to apply more sophisticated and robust adhesive techniques to overcome the weak inherent robustness of superhydrophobic surfaces. Fig. S8 shows the “paint + adhesive (double-sided tape / spray adhesive) + substrates” sample preparation methods (Fig. S8, A and B) and the relevant robustness tests, including finger-wipe (Fig. S8C), knife-scratch (Fig. S8D) and sandpaper abrasion (Fig. S8, E and F). Fig. S9 and Movie S10 show the finger-wipe tests that compare the untreated, paint treated and “paint + double-sided tape” treated (PDT) glass and steel substrates, respectively. After the finger-wipe, the paint directly coated on substrates was removed, while the double-sided tape-bonded paint was still left on the substrates and the surfaces retained superhydrophobicity. Although the inherent robustness of the paint is intrinsically as weak as most superhydrophobic surfaces, it is friendly to adhesives, from which, the robustness was gained. A glass substrate was used as one example for further robustness tests with double-sided tapes (knife-scratch and sandpaper abrasion tests), Movie S10 shows that the glass bonded with double-sided tape and paint still



kept dry and clean after the knife-scratch and then water drop. The sandpaper abrasion tests were carried out on the PDT glass. The PDT glass weighing 100 g was placed face-down to sandpaper (Standard glasspaper, Grit No. 240) and moved for 10 cm along the ruler (Fig. 4A); the sample was rotated by 90° (face to the sandpaper) and then moved for 10 cm along the ruler (Fig. 4B). This process is defined as one abrasion cycle (Movie S11), which guarantees the surface is abraded longitudinally and transversely in each cycle even if it is moved in a single direction. Fig. 4C shows the water contact angles after each abrasion cycle and it was observed that the static water contact angles were between 156 and 168 degrees, indicating superhydrophobicity was not lost by mechanical abrasion. In order to test if this superhydrophobicity was kept after abrasion on the whole area but not merely on some points (contact angle measuring points), water droplet was guided by a needle to travel on the PDT glass surface after the 11<sup>th</sup>, 20<sup>th</sup>, 30<sup>th</sup> and 40<sup>th</sup> cycle's abrasion, respectively (Movie S12). Fig. 4D shows the water droplet travelling after the 40<sup>th</sup> cycle.

To enlarge the application scale and broaden the types of substrates, the spray adhesive (EVO-STIK) was also used to bond glass, steel, cotton wool and filter paper substrates with the superhydrophobic paint. Fig. S10 and Movie S13 show the finger-wipe tests on untreated, paint treated and “paint + spray adhesive” treated (PSAT) substrates, respectively. On hard substrates (glass and steel), PSAT surfaces retained water proofing, while the paint was just removed when directly applied; the case is different on soft substrates (cotton and paper), where paint was protected by their porous structures, resulting in both paint treated and PSAT cotton and paper being superhydrophobic after the finger-wipe. However, in a more powerful test (i.e. sandpaper abrasion of cotton), this “protection” is limited (Fig. S11). Fig. S12 and Movie S14 show that the sandpaper abrasion tests on PSAT substrates, and both hard and soft substrates became robust after the PSAT treatment. Fig. S13 and Movie S15 show that the PSAT substrates retained water repellent after knife-scratch tests. After different damages, the PSAT materials still remained superhydrophobicity, indicating that this method could efficiently enhance the robustness of superhydrophobic surfaces on different substrates; it is believed that the idea of “superhydrophobic paint + adhesives” can be simply, flexibly and robustly used in large-scale industrial applications.

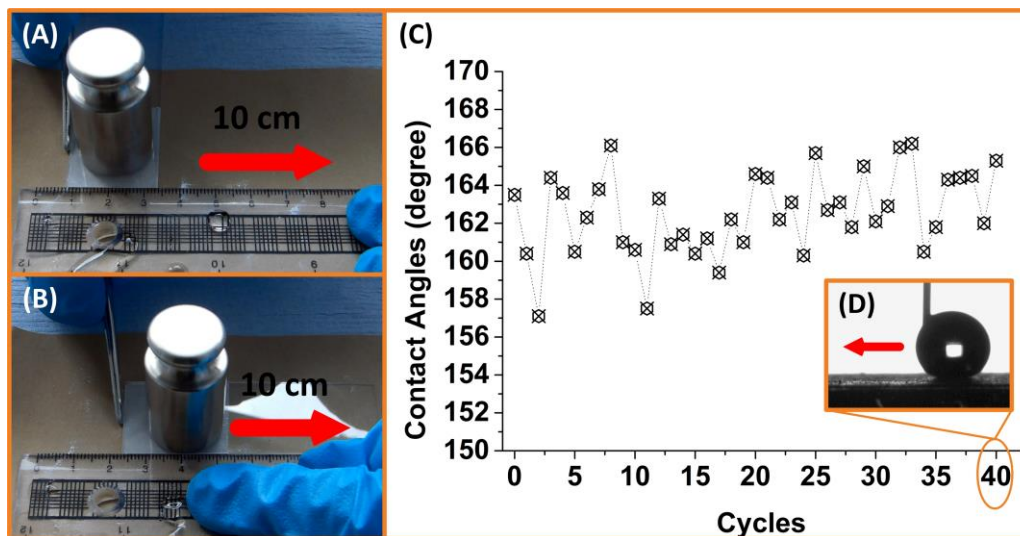


**Fig. 4 Sandpaper abrasion tests.** (A) and (B) show one cycle of the sandpaper abrasion test; (C) the plot of mechanical abrasion cycles and water contact angles after each abrasion test; (D) water droplet travelling test after 40<sup>th</sup> cycle abrasion.

The superhydrophobic surfaces show that a robust resistance to oil contamination and ease of applicability can be achieved by implementing straightforward coating methods such as spraying, dip-coating or even simply extrusion from a syringe. The flexibility of the “paint + adhesives” combination enables both hard and soft substrates to become robustly superhydrophobic and self-cleaning. The surfaces can be readily implemented in harsh and oily environments where robustness is required.

#### References and Notes:

1. W. Barthlott, C. Neinhuis, *Planta* **202**, 1 (1997).
2. R. Blossey, *Nat. Mater.* **2**, 301 (2003).
3. I. P. Parkin, R. G. Palgrave, *J. Mater. Chem.* **15**, 1689 (2005).
4. T. Onda, S. Shibuichi, N. Satoh, K. Tsujii, *Langmuir* **12**, 2125 (1996).
5. L. Feng *et al.*, *Adv. Mater.* **14**, 1857 (2002).
6. J. Zimmermann, F. A. Reifler, G. Fortunato, L. C. Gerhardt, S. Seeger, *Adv. Funct. Mater.* **18**, 3662 (2008).
7. X. Zhu *et al.*, *J. Mater. Chem.* **21**, 15793 (2011).
8. Q. Zhu *et al.*, *J. Mater. Chem. A* **1**, 5386 (2013).
9. A. Tuteja *et al.*, *Science* **318**, 1618 (2007).
10. X. Deng, L. Mammen, H. Butt, D. Vollmer, *Science* **335**, 67 (2012).
11. Y. Lu *et al.*, *ACS Sustainable Chem. Eng.* **1**, 102 (2012).
12. Materials and methods are available as supplementary materials on Science Online.
13. D. Richard, C. Clanet, D. Quéré, *Nature* **417**, 811 (2002).
14. J. C. Bird, R. Dhiman, H. Kwon, K. K. Varanasi, *Nature* **503**, 385 (2013).
15. Y. Lu *et al.*, *J. Mater. Chem. A* **2**, 12177 (2014).
16. D. Vella, L. Mahadevan, *Am. J. Phys.* **73**, 817 (2005).
17. A. Tuteja, W. Choi, J. M. Mabry, G. H. McKinley, R. E. Cohen, *Proc. Natl. Acad. Sci. U.S.A.* **105**, 18200 (2008).
18. A. Nakajima *et al.*, *Langmuir* **16**, 7044 (2000).
19. R. Fürstner, W. Barthlott, C. Neinhuis, P. Walzel, *Langmuir* **21**, 956 (2005).
20. B. Bhushan, Y. C. Jung, K. Koch, *Langmuir* **25**, 3240 (2009).
21. T. Wong *et al.*, *Nature* **477**, 443 (2011).
22. M. Nosonovsky, *Nature* **477**, 412 (2011).
23. A. Grinthal, J. Aizenberg, *Chem. Mater.* **26**, 698 (2014).
24. D. C. Leslie *et al.*, *Nat. Biotechnol.* **32**, 1134 (2014).
25. M. Im, H. Im, J. Lee, J. Yoon, Y. Choi, *Soft Matter* **6**, 1401 (2010).
26. B. Wang *et al.*, *ACS Appl. Mater. Interfaces* **5**, 1827 (2013).
27. M. Horn, C. F. Schwerdtfeger and E. P. Meagher, *Z. Kristallogr* **136**, 273 (1972).
28. Y. Lu *et al.*, *J. Mater. Chem. A*, **2**, 11628 (2014).

#### Acknowledgments:

We thank Martin Vickers and Steve Firth for XRD and TEM characterizations. Thanks to Caroline E. Knapp and Davinder S. Bhachu for ordering chemicals and the help with some experiments.

#### Supplementary Materials:

Materials and Methods

Supplementary Text

Figs S1-S13

Movies S1-S15

References (27-28)